Journal of Alloys and Compounds xxx (2008) xxx–xxx

Contents lists available at ScienceDirect

Journal of Alloys and Compounds

journal homepage: www.elsevier.com/locate/jallcom

Ball-milling in vacuum of α and σ phases of near-equiatomic FeCr alloys

B.F.O. Costa[a,*], G. Le Caër[b], J.M. Loureiro[a]

[a] CEMDRX, Department of Physics, University of Coimbra, P-3004-516 Coimbra, Portugal
[b] Institut de Physique de Rennes, UMR UR1-CNRS 6251, Université de Rennes I, Campus de Beaulieu, Bat. 11A, F-35042 Rennes Cedex, France

ARTICLE INFO

Article history:
Received 30 August 2007
Received in revised form 25 June 2008
Accepted 10 July 2008
Available online xxx

Keywords:
Fe–Cr
α-Phase
σ-Phase
Ball-milling
Amorphisation
Mössbauer spectroscopy

ABSTRACT

The structural changes induced by ball-milling of near-equiatomic σ-FeCr and α-FeCr in vacuum were followed. Besides the α-phase, an amorphous phase appears when milling the σ-phase for times longer than 20 h. An amorphous phase forms too, but at a slower rate than the latter, when milling the α-phase. The partial amorphisation of σ-FeCr and α-FeCr ball-milled in vacuum is concluded to be a phenomenon of intrinsic origin. The amorphous phase crystallizes into a bcc Cr-rich phase and a bcc Fe-rich phase during short annealing steps.

1. Introduction

The broad low-temperature miscibility gap in the central part of the binary Fe–Cr equilibrium phase diagram and the high-temperature σ-phase domain explain the interest for near-equiatomic Fe–Cr alloys. Nearly equiatomic binary Fe–Cr alloys and the multinary alloys derived from them are technologically important materials because of their high-temperature corrosion and mechanical resistance. However, the precipitation of a σ-phase [1,2] makes for instance ferritic stainless steels very brittle (the so-called '475 °C embrittlement').

The behavior under ball-milling of a σ-FeCr phase in vacuum in a vibratory mill was investigated by Bakker et al. [3] who concluded that σ transforms solely into a nanostructured α-FeCr after t_m = 100 h of milling in spite of a low magnetic moment of 1.2 μ_B/Fe atom as compared to an expected moment of ∼2 μ_B/Fe atom for bcc FeCr even nanostructured. The ball-milling of σ-FeCr in argon was studied [4] in conditions similar to theirs. An amorphous phase forms for long t_m in addition to the α-phase. As oxygen favors the formation of an amorphous Fe–Cr phase ([4] and references therein), we followed the structural changes induced by ball-milling of near-equiatomic σ-FeCr and of α-FeCr in vacuum in a Fritsch P0 mill, using Mössbauer spectroscopy as the main characterization technique of the structural changes.

2. Experimental details

A $Fe_{51.8}Cr_{48.2}$ at.% alloy was prepared by melting together in argon atmosphere appropriate amounts of Fe (>99.9% purity) and Cr (99.995% purity) in an induction furnace. The composition, near the center of the σ-phase domain, is close to that studied previously [4]. The σ-phase was formed by annealing the as-cast bcc alloy in vacuum at 700 °C for 100 h. Then, it was powdered with a pestle in an agate mortar into particles of about 90 μm. A bcc $Fe_{49.7}Cr_{50.3}$ at% coarse-grained sample was prepared with a similar procedure. It was smashed and reduced to particles of about 2–3 mm size. Masses of 5 g of σ-FeCr and of α-FeCr were ball-milled in accumulated milling times under vacuum.

Ball-milling was carried out in a Fritsch P0 vibratory mill with a hardened steel vial and a hardened steel ball whose diameter is 5 cm and whose mass is 500 g. The vial cover was home made to permit the coupling to a vacuum pump. The mill was working at its maximum amplitude of vibration (A = 3). A milling cycle consists first in evacuating the vial down to a pressure of 6×10^{-6} mbar and then to mill for 4 h. Cycles are then accumulated to reach the sought-after milling time (≥4 h). The pressure measured at the end of each milling cycle was always better than 10^{-3} mbar. For each set of 5 g of powder, three samples were removed in argon atmosphere at different milling times. Microprobe analyses were used to determine the compositions of the samples.

X-ray diffraction (XRD) was performed at room temperature (RT) using Cu Kα radiation (λ = 0.154184 nm) to characterize the microstructural changes. The mean crystallite size and the microstrain of as-milled samples were obtained from the widths of the XRD peaks using the Williamson–Hall method [5].

^{57}Fe Mössbauer spectra were recorded at RT in a transmission geometry using a standard constant acceleration spectrometer. A ^{57}Co source in Rh matrix with strength of ≈20 mCi was used. The experimental spectra were analysed by a constrained Hesse–Rübartsch method [6], which yields a hyperfine magnetic field distribution (HMFD), $P(B)$. Lorentzian line-shapes were employed in this procedure. As usual, the isomer shifts are given with respect to α-Fe at RT.

Differential scanning calorimetry (DSC) was used to study the transformation of the final as-milled sample during heating in an argon flow from room temperature to 800 °C with a heating rate of 40 °C/min.

* Corresponding author.
E-mail address: benilde@ci.uc.pt (B.F.O. Costa).

0925-8388/$ – see front matter © 2008 Published by Elsevier B.V.
doi:10.1016/j.jallcom.2008.07.179

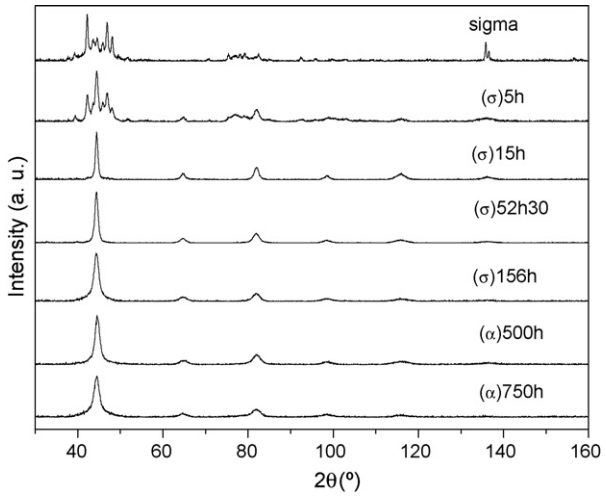

Fig. 1. X-ray diffraction patterns of the sigma (σ) and alpha (α) phase milled for the indicated periods. The top pattern is that of the starting σ-phase.

3. Results and discussion

3.1. Ball-milling of the σ-phase

The composition of the σ-phase milled for a time t_m of 156 h was $Fe_{54.2}Cr_{45.8}$ at.%. The oxygen and nitrogen contents in this sample were 0.7 at.% and 0.04 at.%, respectively. They are less by an order of magnitude than those we obtained previously in argon atmosphere [4] (the oxygen content given in [4] is in wt% and not in at.%) and than those most often reported in the literature for milling in gaseous atmospheres. The measured content suggests that oxygen is preferentially absorbed each time the vial is opened in air to take a sample as observed by Lucks et al. [7]. The iron content increases due to the contamination by the steel of the milling tools.

Fig. 1 shows the XRD patterns as a function of t_m. The intensities of the σ-phase diffraction peaks decrease when t_m increases and the peaks of a bcc phase appear and are already visible after $t_m = 5$ h. After $t_m = 15$ h, the σ-phase is totally transformed. The bcc peaks are broad due to a small average crystallite size and to the effect of strain. The mean crystallite size for $t_m = 156$ h is $\langle d \rangle = 6$ nm and the microstrain is 1%. However, as discussed bellow, a broad diffuse peak due to an amorphous phase is superimposed to the main (1 1 0) peak. The apparent width of the latter peak is consequently larger than the width which would be measured in the absence of an amorphous phase and $\langle d \rangle$ is likely underestimated. From the plateau exhibited by the t_m dependence of $\langle d \rangle$, a reasonable value of $\langle d \rangle$ is ~10 nm.

Fig. 2 shows RT ^{57}Fe Mössbauer spectra and the associated HMFDs for different t_m. The spectrum of the starting σ-phase, which is paramagnetic at RT, is a single broad line with an average isomer shift of −0.18(2) mm/s. A broad magnetic component, due to the magnetic α-phase, appears and its fraction increases with t_m. At 20 h of milling, the shape of the central peak changes. The paramagnetic contribution can no longer be solely attributed to the σ-phase but to another phase whose fraction increases with milling time. At these periods of milling, XRD patterns show no more the σ-phase but only broadened peaks of the bcc phase. The paramagnetic fraction, $A_p(t_m)$, decreases rapidly at a rate of 4.9×10^{-2} h^{-1} until about $t_m = 20$ h, then remains almost constant until $t_m = 60$ h and then increases almost linearly with t_m at a rate of 3.7×10^{-3} h^{-1}. These results are qualitatively similar to those obtained in our previous study of milling of the σ-phase in argon [4].

The average HMF, $\langle B \rangle$, of the magnetic part of a spectrum decreases with milling time and is 16.5(1) T at $t_m = 156$ h. Its isomer shift is $\langle IS \rangle = -0.11$ mm/s while the paramagnetic subspectrum has $\langle IS \rangle = -0.13$ mm/s. The average HMF is calculated first from the published concentration dependence of the average field $\langle B(x) \rangle$ of bcc $Fe_{1-x}Cr_x$ alloys [8] (which were cold-rolled at some stage of their preparation process): $\langle B(x) \rangle = 33.36 - 30.071x - 2.8686x^2$ [8] or $\langle B(x) \rangle = 33.55 - 31.794x$ [9]. We showed in a previous paper [10] that the mean hyperfine fields of concentrated Fe–Cr alloys either filed or ball-milled decrease by about ~2 T whatever the way the alloys are prepared [10]. The hyperfine field calculated from the alloy composition using the previous relations is 19.0(1) T for the σ-phase milled for 156 h. The effect of milling is then expected to decrease that value by about 2 T, yielding thus an expected field of about 17 T, which agrees with the experimental value. The non-magnetic phase can neither be attributed to a σ-phase nor to a bcc phase (see Section 3.2). As diffraction peaks different from those of the bcc phase are not observed on the XRD patterns despite a significant $A_p(156\,h) = 0.49$, we conclude, as we did before for milling in argon, that it is an amorphous phase. The $\langle IS \rangle$'s of the non-magnetic phases are further similar when milling in argon and in vacuum and are, as expected, slightly larger than the isomer shift, ≈−0.17 mm/s, of an amorphous $Fe_{30}Cr_{70}$ thin film [11].

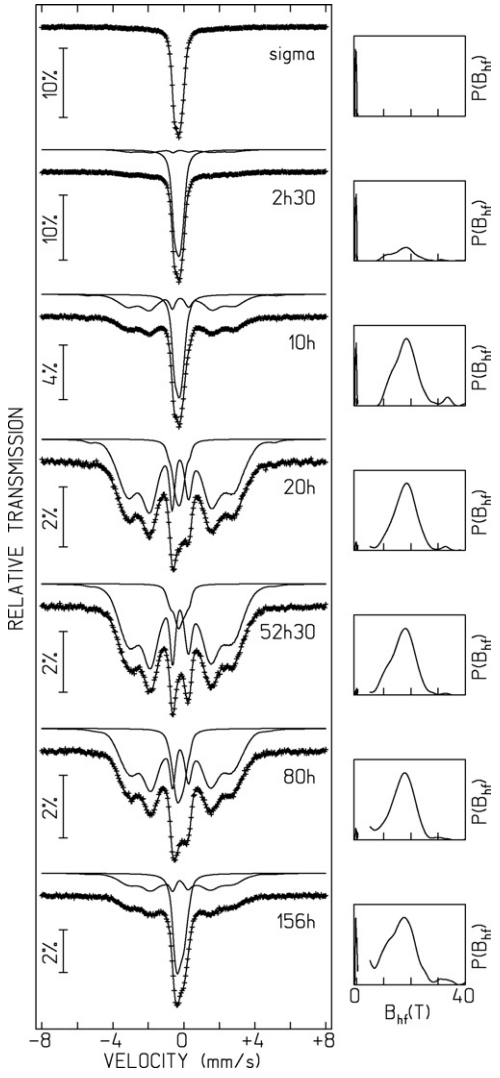

Fig. 2. RT ^{57}Fe Mössbauer spectra of the σ-phase and HMFD's as a function of milling time.

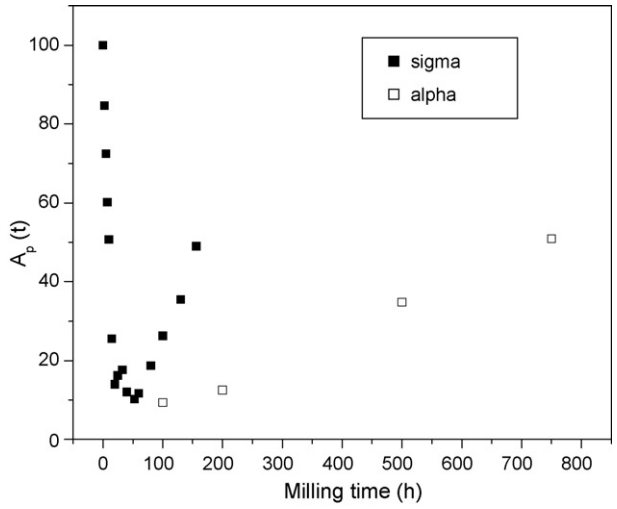

Fig. 3. Paramagnetic fraction $A_P(t)$ measured from the RT Mössbauer spectra of the σ and α phases milled for the indicated periods.

The XRD patterns of amorphous phases obtained by thermal evaporation [11] exhibit only a very broad first halo whose maximum is very close to that of the (1 1 0) bcc peak, a halo that would be hard to evidence when a broadened (1 1 0) peak is superimposed on it. In otherwise the same milling conditions, the amorphous phase forms more rapidly, $A_p(80\,h) = 0.34$, when milling in argon, than when milling in vacuum, $A_p(80\,h) = 0.19$, with a much larger oxygen content in the former case than in the latter [4]. In both cases, the $A_p(150\,h)$'s are alike ∼0.5. Amorphisation appears thus as being an intrinsic phase transformation of the α-phase originating from the σ-phase in our conditions of injected power and not only a transformation essentially dependent on a significant oxygen contamination. As $A_p(100\,h)$ is ≈0.3 (Fig. 3), the average moment per atom is estimated to be $\approx 0.7 \times 2 = 1.4\ \mu B$/at. because the amorphous phase is non-magnetic even at low temperature [11]. It is close to the average moment, 1.2 μ_B/at., reported by Bakker et al. [3] for a σ-phase ball-milled for 100 h in rather similar milling conditions. This rather low moment value, which was attributed to a sole bcc phase [3], is actually that of a mixture of a bcc phase and of an amorphous phase which escapes detection by X-ray diffraction because its first intense halo is hidden by the main (1 1 0) bcc line.

The final sample was annealed to crystallize the amorphous phase. Two exothermic peaks associated to a crystallization process are observed at 600 and 680 °C on the DSC trace of the sample milled for 156 h, as found too for argon milling [4]. The sample was annealed at $T_{a1} = 600$ °C for 6 min. After having been characterized, it was further annealed at $T_{a2} = 680$ °C for 6 min. XRD patterns are those of bcc phases. Mössbauer spectra (Fig. 4) show the crystallization of a Fe-rich phase (a) and of a Cr-rich phase (b). The magnetic component, with a rather large field, is associated with a Fe-rich bcc alloy. The central paramagnetic component is associated with a Cr-rich bcc alloy as the Curie temperature of $Fe_{1-x}Cr_x$ alloys decreases with x and becomes lower than 300 K at $x > \sim 0.66$ [12]. Further, a Cr-rich phase must be formed because the Fe-rich phases formed during annealing have Fe contents larger than the average content of the alloy (see below). The hyperfine parameters are $\langle B \rangle = 22.0(2)$ T and $\langle IS \rangle = -0.094$ mm/s for the spectrum recorded after the first annealing (Fig. 4a). After the second annealing, $\langle B \rangle = 25.5(2)$ T and $\langle IS \rangle = -0.081$ mm/s for the magnetic component and $\langle IS \rangle = -0.087$ mm/s for the paramagnetic one (Fig. 4b). From the relations $\langle B(x) \rangle$ given above, we obtain the Cr contents of 36.0(5) at.% and 25.5(5) at.%, respectively from the average fields. As the latter Cr content is significantly lower than the Cr content of the alloy (45.8 at.%), a phase separation occurs, either in the amorphous state or during the crystallization stage, a conclusion confirmed by the observation of a paramagnetic peak associated with a Cr-rich phase after the second annealing with $A_p(T_{a2} = 680\,°C) = 8.6\%$. Assuming equal Lamb–Mössbauer factors for the two bcc phases, we estimate their final compositions as $Fe_{74.5}Cr_{25.5}$ and $Fe_{14}Cr_{86}$, respectively. Such a Cr-rich phase is antiferromagnetic with a Néel temperature close to 100 K. The very small lattice parameter variation of bcc Fe–Cr alloys with the Cr content explains that a single set of bcc peaks is observed on XRD patterns after crystallization.

3.2. Ball-milling of the α-phase

The composition of the α-phase ball-milled for 100 h, 500 h and 750 h is $Fe_{54.5}Cr_{45.5}$ at.%, $Fe_{56.7}Cr_{44.3}$ at.% and $Fe_{58.6}Cr_{41.2}$ at.%, respectively and the oxygen content is 0.2 at.%, 0.7 at.% and 0.8 at.%, respectively. The iron content increases because of steel contamination but the oxygen content remains small even after 750 h of milling. Fig. 1 shows the XRD pattern for the sample milled for 750 h made only of broadened bcc peaks. The sample milled for 750 h has an apparent grain size of 6 nm and a microstrain of 1.6% (see Section 3.1).

^{57}Fe Mössbauer spectra and HMFD's of milled samples are shown in Fig. 5 for the indicated periods. An amorphous phase forms too, but at a much slower rate than in the previous case (Fig. 3). The area fraction $A_p(t_m)$ increases linearly with t_m at a rate of $6.7 \times 10^{-4}\ h^{-1}$, that is 5.5 times slower than for the σ-phase (Section 3.1). The average HMF of the magnetic part of the spectra is almost constant during milling, $\langle B \rangle \approx 17.6$ T and $\langle IS \rangle = -0.096$ mm/s. The $\langle IS \rangle$ of the paramagnetic subspectrum is −0.078 mm/s. As explained above, the calculated field is 17.5(2) T for the starting alloy and is 20.0(4) T from the compositions of alloys milled for 500 h and longer. As milling decreases the field by about ∼2 T [10], the expected field of ∼18 T agrees with experiment. The bcc phase milled for 500 h, with a grain size of ∼10 nm, is ferromagnetic among others because nanograins are magnetically coupled in micron-sized particles. Its composition deduced from its HMF is consistent with that obtained from microprobe analysis. Therefore, the paramagnetic component cannot originate from a nanostructured bcc Cr-rich paramagnetic phase at RT whose Cr content would have to be larger than ∼66 at.% ($T_c(0.66) \approx 300$ K [12]). The central paramagnetic component is then attributed to an amorphous phase. For 500 h of milling, the oxygen content is 0.7 at.% and $A_p(500\,h) = 0.35$. The oxygen content of the sample milled for 750 h is nearly the same, 0.8 at.%, but the amorphous fraction is now $A_p(750\,h) = 0.51$. The amorphisation process is concluded as above to be an intrinsic phenomenon. Although the faster amorphisation kinetic of the σ-phase ball-milled in vacuum as compared to that of the α-phase ball-milled in identical conditions is still unexplained,

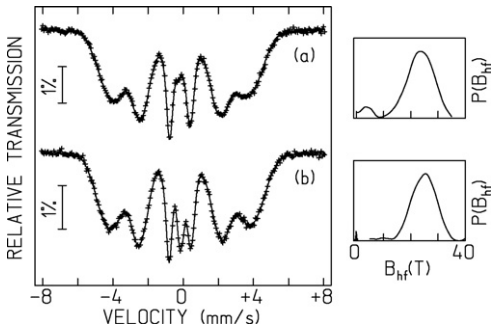

Fig. 4. RT ^{57}Fe Mössbauer spectra of the σ-phase milled for 156 h and annealed at (a) 600 °C for 6 min; (b) 600 °C for 6 min and then at 680 °C for 6 min.

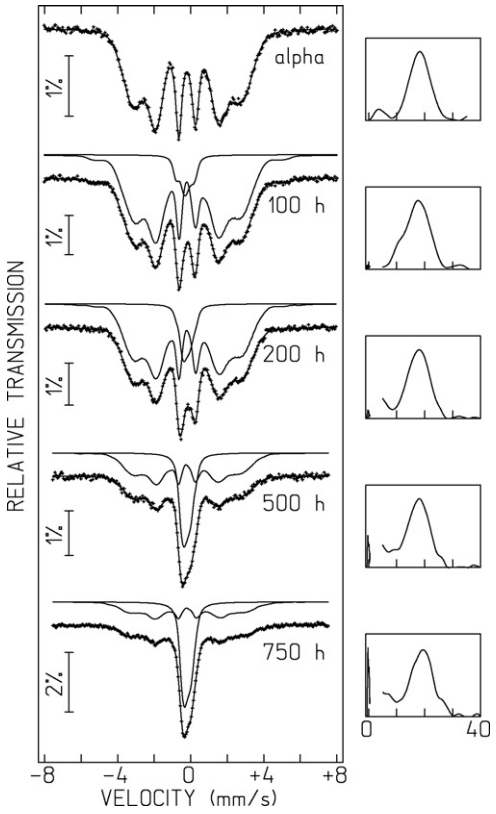

Fig. 5. RT ^{57}Fe Mössbauer spectra of the α-phase and HMFD's as a function of milling time.

a contribution to that speed-up of the differences in oxygen contents cannot be fully excluded even if the latter remain low in both experiments.

The sample milled for 500 h was similarly annealed at $T_{a1} = 600\,^{\circ}C$ and $T_{a2} = 680\,^{\circ}C$. XRD patterns only show the peaks of bcc phases. After the first annealing, $\langle B \rangle = 21.0(2)$ T, $\langle IS \rangle = -0.068$ mm/s while, after the second annealing, $\langle B \rangle = 23.1(2)$ T, $\langle IS \rangle = -0.056$ mm/s for the magnetic component and $\langle IS \rangle = -0.031$ mm/s for the paramagnetic one. The Cr contents calculated from the average fields are 39.5(5) at.% and 33.0(5) at.%, respectively. The composition of the Cr-rich phase can be estimated from the average alloy composition, $Fe_{56.7}Cr_{44.3}$, the composition of the Fe-rich phase, $Fe_{67}Cr_{33}$, and the area fraction $A_p(T_{a2}) = 5.1\%$ which means that 5.1% of all the Fe atoms are in that Cr-rich phase. In summary, the compositions of the Fe-rich and Cr-rich bcc phases are obtained to be $Fe_{67}Cr_{33}$ and $Fe_{14}Cr_{86}$, respectively.

4. Conclusions

The structural changes induced by ball-milling of near-equiatomic σ-FeCr and α-FeCr in vacuum in a Fritsch P0 mill were followed. Besides the α-phase, an amorphous phase appears when milling the σ-phase for times longer than 20 h. An amorphous phase forms too, but at a slower rate, when milling the α-phase. As the oxygen contents are small, the partial amorphisation of both σ-FeCr and of α-FeCr ball-milled in vacuum is concluded to be an intrinsic phenomenon which does not necessarily need the presence of residual gases but requires the appropriate injected power as discussed in [4]. That conclusion is consistent with the formation of amorphous alloys in $Fe_{1-x}Cr_x$, $0.40 < x < 0.75$, by coevaporation in a vacuum of 3×10^{-7} Torr [11]. By comparison with results obtained in similar milling conditions but with a much higher oxygen content [4], oxygen is concluded to increase the amorphisation rate although it does not seem to change the final amorphous fraction. A partial amorphisation accounts too for the low value of the saturation magnetization, 1.2 μ_B/at., measured by Bakker et al. [3] for an as-milled σ-phase. A crystallization of the amorphous phase into in a bcc Cr-rich and a bcc Fe-rich bcc phase occurs by short annealing.

Acknowledgements

This work was partially supported by FCT and FEDER European funds (Grant No. POCTI-SFA-2-30, Portugal). The financial support of the Portuguese–French bilateral program PESSOA is also gratefully acknowledged.

References

[1] O. Kubachewski, Iron-Binary Phase Diagrams, Springer, Berlin, 1982, p. 185.
[2] S.M. Dubiel, G. Inden, Z. Metalkd. 78 (1987) 544–549.
[3] H. Bakker, H. Zhou, G.F. Yang, Prog. Mater. Sci. 39 (1995) 159–241.
[4] B.F.O. Costa, G. Le Caer, J.M. Loureiro, V.S. Amaral, J. Alloys Compd. 424 (2006) 131–140.
[5] G. William, W.H. Hall, Acta Metall. 1 (1952) 22–31.
[6] G. Le Caer, J.M. Dubois, J. Phys. E 12 (1979) 1083–1090.
[7] L. Lucks, P. Lamarter, E.J. Mittemeijer, Acta Mater. 49 (2001) 2419–2428.
[8] S.M. Dubiel, J. Zukrowski, J. Magn. Magn. Mater. 23 (1981) 214–228.
[9] D. Chandra, L.H. Schwartz, Met. Trans. 2 (1971) 511–519.
[10] P. Delcroix, G. Le Caër, B.F.O. Costa, J. Alloys Compd. 434–435 (2007) 584–586.
[11] S.K. Xia, E. Baggio-Saitovitch, C. Larica, Phys. Rev. B 49 (1994) 927–931.
[12] S.K. Burke, R. Cywinski, J.R. Davis, B.D. Rainford, J. Phys. F: Met. Phys. 13 (1983) 451–470.